Collaborative subcellular compartmentalization to improve GPP utilization and boost sabinene accumulation in *Saccharomyces cerevisiae*

Hongjie Jia
Tianjin University
Tianhua Chen
Tianjin University
Junze Qu
Tianjin University
Mingdong Yao
Tianjin University
Wenhai Xiao
Tianjin University
Ying Wang (ying.wang@tju.edu.cn)
Tianjin University https://orcid.org/0000-0003-2311-015X
Chun Li
Beijing Institute of Technology
Yingjin Yuan
Tianjin University

Research

Keywords: compartmentalization, mitochondrial morphology, GPP, sabinene, Saccharomyces cerevisiae

Posted Date: February 18th, 2020

DOI: https://doi.org/10.21203/rs.2.23800/v1

Version of Record: A version of this preprint was published at Biochemical Engineering Journal on December 1st, 2020. See the published version at https://doi.org/10.1016/j.bej.2020.107768.

Abstract

Background Monoterpenes and their derivatives play an important role as flavorings, perfume additives, pharmaceuticals and advanced biofuels. GPP (geranyl diphosphate) is the direct precursor to biosynthesize this class of products. The present study for monoterpenes synthesis in yeast focused on manipulation of metabolic flux to improve GPP supply. However, if the subcellular distribution of GPP and monoterpene synthase were not coincided with each other, it would be hard to well utilize GPP, leading to a waste of carbon sources.

Results Herein, we took sabinene production in *Saccharomyces cerevisiae* as an instance, and confirmed the location of N-truncated sabinene synthase (t34SabS1) in yeast cytosol (C). We also revealed the existence of GPP pools in organelles [such as lipid monolayer membrane-bound peroxisomes (P) and bilayer membrane-bound mitochondria (M)] beside cytosol. In order to minimize the loss of GPP, an engineering strategy was proposed to coordinated compartmentalization of sabinene synthase. Initially, expression of t34SabS1 in an ERG20-downregulated host only obtained 19.4 mg/L sabinene. Combined targeting t34SabS1 into CM (cytosol and mitochondria) increased sabinene production to 64.6 mg/L. This titer was significantly higher than those generated by harnessing other combinations of subcellular locations (i.e. CP, PM and even CPM). Further overexpression of the genes involved in mitochondria morphology uncovered four novel molecular targets (i.e. FIS1 , LSB3 , MBA1 and AIM25) associating with sabinene output. Especially, overexpression of AIM25 enhanced the sabinene production to 90.4 mg/L. Eventually, integrating all above engineered genes into host chromosome achieved 154.9 mg/L of sabinene.

Conclusions The engineering approaches of this study improve GPP utilization and boost sabinene accumulation almost 60-fold of the original titer. This research highlights the strategy of organelle engineering to improve precursor utilization and to enhance the compartmentalized pathway. It also sets a good reference to synthesize other valuable monoterpenes and their derivatives in eukaryotic hosts.

Background

Monoterpenes play an important role as flavorings, perfume additives, pharmaceuticals and advanced biofuels [1–3]. At present, extraction from plants remain the main source to manufactory these valuable products, which cannot meet the increasing market demand and prompt heterologous bioproduction an important complement to the traditional modes [4, 5]. Monoterpenes are directly converted from geranyl diphosphate (GPP) by monoterpene synthase. In eukaryotic hosts like Saccharomyces cerevisiae, GPP is generated from isopentenyl pyrophosphate (IPP) and dimethyl allyl pyrophosphate (DMAPP) by farnesyl diphosphate synthase (ERG20) located in cytosol (C) (Fig. 1). However, the native ERG20 transforms most GPP into farnesyl diphosphate (FPP) to produce endogenous isoprenoid compounds (like sterols) essential for cell viability [6]. Therefore, the frequently adopted method for monoterpene synthesis in yeast is to enlarge GPP pool without abolishing FPP flux channeled directly from IPP and DMAPP. These validated strategies include ERG20 mutagenesis [e.g. $ERG20^{WW}$ ($ERG20^{F96W/N127W}$)] [7] as well as down-

regulation of native ERG20 by inducible weak promoter [8] or N-degron dependent protein degradation [9]. Ignea et al. [4] even set up an orthogonal pathway to generate the cis-isomer of GPP, i.e. neryl diphosphate (NPP), to provide sufficient substrates for monoterpene synthase. Even though above strategies have achieve remarkable improvements on monoterpenes biosynthesis, it seldom discusses the question that whether the enhanced GPP pools can be well utilized?

Yeast has many subcellular organelles, and each organelle offers a unique physiochemical condition (e.g. pH, metabolites, cofactors, etc.) for its favorable enzymatic reaction(s) [10]. Harnessing the metabolic flux in subcellular compartments proved great benefits as higher local concentrations of substrates and enzymes, lower intermediate cytotoxicity as well as fewer by-products [11]. These advantages have increased the biosynthesis level of series products [12, 13], making the possibility of organelle engineering become one of the important advantages of eukaryotic hosts, compared to prokaryotic ones. However, the existence of organelles also bring the issue of subcellular distribution of the key enzyme and its substrate. On one hand, for monoterpene synthase, the N-terminal transit peptide directs the enzyme to plastid in its nature hosts [14, 15]. When expression of the full-length monoterpene synthase in S. cerevisiae lacking the mechanism of plastid targeting, it is unclear where the monoterpene synthase located. Moreover, some monoterpene synthases were expressed in their N-truncated mature forms to gain improved expression levels as well as enhanced catalytic activities [16]. Jiang et al. [17] once pointed out that N-truncated geraniol synthase was located in cytosol. However, other N-truncated monoterpene synthases might not follow the same laws, since truncation of the disorder structure has not always brought to soluble expression in cytosol. For instance, the N-truncated heterologous CYP11A1, adrenodoxin and adrenodoxin reductase were detected at plasma membrane, cytosol and endoplasmic reticulum of S. cerevisiae, respectively [18]. Thus, the distribution of monoterpene synthase is still need to be investigated.

On the other hand, for GPP which synthesized in yeast cytosol, the distribution of this compound is also unclear. But the activity of yeast mitochondrial geranylgeranyl diphosphate synthase [19] indicates the presence of a significant pools of C_5 (IPP and DMAPP) and C_{15} units (FPP) in yeast mitochondria (M). Farhi et al. [12] also once gained high production level of valencene and amorphadiene, when targeting heterologous sesquiterpene synthases to mitochondria as well as introducing all the enzymes downstream of DMAPP and IPP (ERG20 and sesquiterpene synthases) into mitochondria. Thus, according the subcellular distribution of the analogues C_5 and C_{15} units in yeast, it rises a speculation that there might also be a sufficient pool of C_{10} units (GPP) in mitochondria and even other organelles besides cytosol. We noticed that the lipid membranes enclosed those organelles might also limits GPP inside, since Yee et al. [5] once realized a significant increase on geraniol production in S. cerevisiae by targeting the whole biosynthetic pathway from acetyl-CoA into mitochondria to protect GPP from consumption by the cytosolic ergosterol pathway. If the subcellular distribution of GPP and monoterpene synthase were not coincided with each other, it is hard to well utilize GPP to generate monoterpenes, leading to a great waste of carbon sources. Therefore, the distribution of GPP is also need to be

investigated, which would guide us to design the compartmentalization of monoterpene synthase, for the utilization of GPP dispersing within yeast organelles in addition to the cytosolic supply (Fig. 1).

Herein, we take the synthesis of sabinene [a high value and complex bicyclic monoterpene [20]] in S. cerevisiae as an example to investigate the subcellular location of sabinene synthase and GPP, as well as to explore GPP utilization strategy. To gain high expression level and catalysis activity of sabinene synthase, we test the proper truncation position and adopted the N-truncated one (t34SabS1) from Salvia pomifera to establish the sabinene synthetic pathway in our former constructed host. In the meanwhile, mutated ERG20^{WW} was introduced as well as the wild-type ERG20 was downregulated (Fig. 1) to guarantee a promising GPP supply. Through compare the distribution pattern of free green fluorescent protein (GFP) with t34SabS1, we proved t34SabS1 was located within cytosol. By compared the sabinene output generated by individually peroxisomes (P), mitochondria or cytosol targeted t34SabS1, we also identified GPP pools in yeast membrane-bound organelles besides cytosol. Based on above data, a collaborative subcellular compartmentalization strategy was proposed to combined targeting t34SabS1 into different location combinations (i.e. CP, CM, PM and CPM) to coordinated converse GPP into sabinene. Then the output of this compartmentalized pathway was further improved by modifying the morphology (e.g. size, number, shape, etc.) of the related organelle(s). Eventually, integrating all above engineered genes into the host chromosome generate 154.9 mg/L of sabinene which was almost 60-fold of our original titer. This work provided considerable potential for further improving the monoterpene biosynthesis in yeast.

Results

Construction of sabinene synthetic pathway in S. cerevisiae

Initially, sabinene synthetic pathway was established on centromeric plasmid-based system (Additional file 1: Fig. S1a). The sabinene synthase (SabS1) from S. pomifera, which was reported to demonstrate better catalytic specificity than those from other sources [21], was chosen and introduced along with ERG20^{WW} into our former constructed strain YJGZ1 [17] (Fig. 2a). Based on this host harboring overexpressed tHMGR (truncated 3-hydroxy-3-methylglutaryl-coenzyme reductase) and IDI1 (isopentenyl diphosphate isomerase) (Fig. 2a), a gram grade titer of geraniol has been achieved [17], which would guarantee a promising GPP supply for sabinene production. In the meanwhile, yeasts derived from strain YJGZ1 (△GAL80 background) adopt inducible GAL promoters to control heterologous genes (Additional file 1: Fig. S1a). In that case, the fermentation process would be divided into cell growth stage and sabinene accumulation stage, to relieve the cytotoxicity brought by sabinene. Also to reduce product toxicity, 20% (v/v) isopropyl myristate (IPM) was supplemented into the culture before fermentation to enrich sabinene. As shown in Additional file 1: Fig. S2, the products of the initial sabinene producing strain Sc041001 and its parental strain YJGZ1 (Control) were analyzed by GC-TOF-MS after 96-h cultivation. For strain Sc041001, it was detected a chromatographic peak whose retention time (3.99 min) as well as the mass fragment (91, 93, 136 m/z) were consistent with those of the sabinene standard,

respectively, while no such peak was detected in the control (Additional file 1: Fig. S2). This data indicated that the sabinene biosynthesis pathway was successfully functioned in S. cerevisiae.

The N-terminal transit peptide of monoterpene synthetase is proteolyzed after targeting to plastid [14, 15]. When expression of the full-length ones in S. cerevisiae, it might result in reduction of enzyme activities due to the lack of plastid targeting and cutting mechanism of transit peptides. In order to further increase sabinene titer, sabinene synthase was attempted expressed in their N-truncated mature forms, and the proper truncation position was investigated according to the putative disordered region of SabS1 (M1-R43, Additional file 1: Fig. S3) predicted by the PSIPRED Workbench (http://www.cbs.dtu.dk/services/Chlorop/). As shown in Fig. 2b, SabS1 was truncated at three different positions within its N-terminus (i.e. L34, R43 and L52), generating proteins t34SabS1, t43SabS1 and t52SabS1, respectively. These three N-truncated SabS1 were introduced into strain YJGZ1 to measure their corresponding sabinene output. Besides, each N-truncated SabS1 was further fused with RFP and expressed in strain YJGZ1 to determine their expression level. As a result, compared with the full-length SabS1, these three ways of N-truncation did not weaken the expression level of SabS1 (Fig. 2c). However, none sabinene could be detected in the strains harboring t43SabS1 or t52SabS1 (Fig. 2c). That might due to the damage to the $RR(X)_8W$ motif (R43-W53 within SabS1, Additional file 1: Fig. S3) which is highly conserved among most of monoterpene synthetases and is critical to their catalytic activities [14]. Whereas, among those tested SabS1s, t34SabS1 achieved the highest sabinene production as well as the highest expression level, which were increased by 99.2% (reach to 5.28 mg/L) and 96.1% than the sabinene titer and the RFU (relative fluorescence units) of the strains harboring the full-length SabS1, respectively (Fig. 2c). This data suggested that truncation at L34 not only improve the expression level of soluble proteins, but also be benefit to its catalytic activity. Further dynamically down-regulated the transcription of wild-type gene ERG20 via replace the endogenous promoter of ERG20 by glucose-dependent weak promoter HXT1, increased the sabinene titer by 2.67-flod (to 19.4 mg/L, Fig. 2d). Correspondingly, the wild-type ERG20 in the host strain YJGZ1 was also down-regulated to generated strain YCTH1 for further optimization.

Investigation of the subcellular location of sabinene synthase and GPP

Yeast has many subcellular organelles, each of which has a unique physiological environment and cofactors to support different metabolic pathways [22]. Among these organelles, peroxisomes and mitochondria represent the typical ones enclosed by lipid monolayer and bilayer membranes, respectively. Both of these two organelles are rich in cofactors (like ATP and NADPH) for terpene synthesis. Notably, according to Liu et al. [23], the peroxisomal lumen was consider as an efficient site for reactions involved hydrophobic chemicals like fatty acids. Through harnessing peroxisomes as subcellular compartments for triterpenes synthesis, they dramatically increase squalene titer to an extremely high level [23]. Besides, the detoxification function of peroxisomes might be helpful to produce the cytotoxicity brought by monoterpenes. Thus, peroxisomes might suit monoterpene synthesis. Meanwhile, the high pH

environment in mitochondria might be benefit to formation and maintain the critical carbocation intermediate within the reaction catalyzed by monoterpene and sesquiterpene synthase [24]. Farhi et al. [12] once reported that individually overexpression of valencene synthase or amorphadiene synthase in yeast mitochondria gained much more valencene and amorphadiene production than overexpression in the cytosol, suggesting that mitochondria provide a preferable environment for activities of sesquiterpene synthase. Correspondingly, the catalytic environment mitochondria might also be benefit to monoterpene synthase. Therefore, peroxisomes and mitochondria were select as the candidate organelles for sabinene production.

As known, free GFP expressed in yeasts usually uniformly dispersed in cytosol [25]. When introducing GFP into the strain harboring RFP fused t34SabS1, the overlapping green and red fluorescence signals observed by confocal laser scanning microscope indicated that t34SabS1 was located at cytosol (Fig. 3a). This cytosolic protein is hard to attach any precursor enclosed by organelle membranes. If GPP could pass through lipid membranes to form enough precursor pools in peroxisomes and mitochondria, simply expressing t34SabS1 in these two organelles would obtain satisfactory sabinene output. As reported, the signal peptides SKL (GGGSSKL) [26] and MLS (LSLRQSIRFFKPATRTLCSSRYLLQ) [27] have been successfully used to locate enzymes to peroxisomes and mitochondria, respectively. Here, these two protein-targeting signals were adopted and individually attached to the C-terminal and N-terminal of t34SabS1, respectively, and then expressed in strain YCTH1 in a fully chromosome integrated form (Additional file 1:Fig. S1c), while gene $ERG20^{ww}$ was carried by centromeric plasmid. In order to verify whether SKL or MLS fused t34SabS1 was targeting into the desired location, RFP was directly fused to the C-terminal of t34SabS1 (Additional file 1: Fig. S1d). And the GFP fused PEX3 [28] and COX4 [29] were co-expressed with t34SabS1–RFP as the specific marks of peroxisomes and mitochondria, respectively. As demonstrated by fluorescence microscopy, SKL and MLS directed t34SabS1s appeared shapes of dots and rings, respectively, which were consistent to the reported typical patterns of peroxisomes [26] and mitochondria [27], and overlapped with the corresponding specific markers (Fig. 3a). Thus, t34SabS1–SKL and MLS–t34SabS1 were successfully located in peroxisomes and mitochondria, respectively. In terms of sabinene production, unanticipated, expression of peroxisomal (P) or mitochondrial (M) t34SabS1 was not demonstrated significantly superior to utilization of cytosolic (C) t34SabS1 (Fig. 3b). Targeting t34SabS1 to peroxisomes or mitochondria achieved comparable titer to the one produced by cytosolic t34SabS1 (Fig. 3b). This data confirmed the existence of GPP pools in peroxisomes and mitochondria. And these parts of GPP should be utilized for sabinene production in addition to the cytosolic supply.

Combined subcellular compartmentalization of sabinene synthase

Subcellular targeting the key enzyme towards precursor storage location has been proved to be promising to achieve high level production. Lv et al. [27] once promote the synthesis of isoprene in S. cerevisiae through dual metabolic engineering of cytoplasmic and mitochondrial acetyl-CoA. Yang et al. [25] obtained highly effectively compartmentalized biosynthesis of triacylglycerol derived products in

Yarrowia lipolytica via simultaneously targeted lipase dependent pathways directed towards three lipid related organelles. Herein, in order to realize adequate utilization of the GPP pools dispersed within the cell, t34SabS1s were tempted to be simultaneously targeted to different combination of locations. Firstly, three strains were constructed, i.e. strain Sc041063 for targeting t34SabS1 to cytosol as well as peroxisomes (CP), strain Sc041064 for targeting to cytosol as well as mitochondria (CM) and strain Sc041066 for targeting to peroxisomes as well as mitochondria (PM). As a result, all the stains harnessing double subcellular locations (CP, CM and PM) made significantly higher sabinene output than those achieved by cytosolic t34SabS1 with the same copy numbers (Fig. 3c). Among these constructed strains, strain Sc041064 (CM) gained the highest sabinene titer of 64.6 mg/L, which was 85.1% and 79.9% higher than those of strain Sc041063 (CP) and strain Sc041066 (PM), respectively (Fig. 3c). And this sabinene titer for CM was 1.53-fold and 1.73-fold higher than those of strains Sc041065 and Sc041067 with double copies of t34SabS1s in cytosol and mitochondria, respectively (Fig. 3c). However, supplement of another copy of peroxisomal t34SabS1 into strain Sc041064 (obtaining strain Sc041069 for CPM) could not further improve sabinene output, and even resulted in the larger errors on sabinene production (Additional file 1:Fig. S4), suggesting strain Sc041069 was extreme instability. That probably was due to the cell burden brought by high level expression of t34SabS1 in three subcellular location. And mitochondria might be sensitive in such case because them involved in energy supplies and central metabolism which are all vital to yeast survival [30]. Thus, strain Sc041064 harboring cytosolic and mitochondrial t34SabS1 was adopted for further optimization.

Regulation of mitochondria dynamics

Low capacity for substrates/enzymes is a limitation for many organelles [31]. Increasing local concentrations of substrates/enzymes in organelles may results in faster reaction rates and higher productivity. Through combining overexpression of PEX34 and deletion of PEX31 and PEX32, Zhou et al. [31] increased the peroxisome population and improve alkane production by 2-fold. This shows that genetically control cellular physiology to alter organellar number, volume and shape is critical to enhance the compartmentalized pathway. In our case, double the copy number of mitochondrial t34SabS1 did not alter the sabinene titer (Fig. 3b and 3c), indicating the concentration of GPP in mitochondria tended to be saturation relative to the concentration of mitochondrial t34SabS1. Thus, we should tempt to enlarge the number, size or dispersion of mitochondria to improve sabinene synthesis.

Biogenesis, growth and division of organelles are highly controlled by different mechanisms. In yeast, mitochondrial morphology depends on its dynamic behavior (called mitochondrial dynamics) including continuously move along cytoskeletal tracks as well as frequently balancing between fusion (interconnected networks) and fission (distinct small spherical particles) activities [32, 33]. Mitochondrial dynamics are important for their metabolism and many important functions. In order to attempt to improve sabinene production via altering mitochondrial morphology, ten proteins associated with mitochondrial dynamics (Table 1) were selected and individually overexpressed in their centromeric plasmid-based form in the t34SabS1 CM-targeted strain. These overexpressed proteins covered FIS1 [34] for mitochondrial division; MGM1 [35] for mitochondrial fusion; MMM1 [36] and SNF1 [37] for

mitochondrial tubulation; ARC18 [38], LSB3 [39] and JSN1 [40] for mitochondrial motility; as well as other functional protein like GEM1 [41], MBA1 [42] and AIM25 [43]. Among these proteins, only overexpression of FIS1, LSB3, MBA1 and AIM25 significantly enhanced sabinene production (Additional file 1: Fig. S5).

Table 1
Proteins involved in mitochondrial dynamics

Process	Protein	Systematic Name	Proposed function	Reference
Division	FIS1	YIL065C	Mitochondrial fission protein, assembles with DNM1 and MDV1 into a ternary complex that mediates mitochondrial outer membrane division.	[34]
Fusion	MGM1	YOR211C	Mitochondrial GTPase, presents in complex with UGO1 and FZO1, required for mitochondrial inner membrane fusion.	[35]
Tubulation	MMM1	YLL006W	A member of ER-mitochondria encounter structure, assembles with MDM10 and MDM12 into a ternary complex in mitochondrial outer membrane for maintenance of mitochondrial DNA nucleoids and mitochondrial tubular shape.	[54]
	SNF1	YDR477W	AMP-activated protein kinase in response to glucose depletion, involved in mitotic spindle alignment along the mother-bud axis.	[37]
Motility	ARC18	YLR370C	Subunit of the actin-related proteins ARP2/3 complex, required for actin polymerization-driven mitochondrial motility.	[38]
	JSN1	YJR091C	RNA-binding proteins on the mitochondrial surface, co-localizes with ARP2/3 complex and supports them targeting to mitochondria.	[40]
	LSB3	YFR024C	Binding to LAS17 which involved in actin patch assembly and actin polymerization.	[39]
Other	GEM1	YAL048C	Outer mitochondrial membrane GTPase, a member of ER-mitochondria encounter structure, requires for maintenance of mitochondrial morphology.	[41]
	MBA1	YBR185C	Mitochondrial ribosome-binding protein localizes to mitochondrial inner membrane, involved in organization of the mitochondrial inner membrane and required for assembly of mitochondrial respiratory chain complexes.	[42]
	AIM25	YJR100C	Mitochondrial protein involved in the regulation of chronological lifespan, and responses to both heat shock and oxidative stress, required for maintaining the integrity of the mitochondrial network.	[43]

As demonstrated in Additional file 1: Fig. S6, overexpression of FIS1, LSB3, MBA1 and AIM25 did not affect cell growth, indicating these alternations on mitochondrial morphology did not damage the energy metabolism and central carbon metabolism in mitochondria. In order to determine the expression level of t34SabS1 located in cytosol and mitochondria, RFP was individually fused with the tested proteins expressed in these two locations. In the meanwhile, the mitochondria within the strains harboring RFP fused mitochondria t34SabS1 was specifically dyed by Rhodamine 123 [44]. As shown in Fig. 4b, when individual overexpression of FIS1, LSB3, MBA1 and AIM25, MLS–t34SabS1 still located only in mitochondria. Before tuning mitochondrial morphology, there was no significant difference between the expression level of cytosol and mitochondria-targeted t34SabS1 (Fig. 4a). And individual overexpression of these four proteins did not significantly altered the ratio between cytosol and mitochondria-targeted t34SabS1 (Fig. 4a), suggesting tuning mitochondrial morphology did not affect protein subcellular localization and expression level.

FIS1 is a mitochondrial fission protein mediating mitochondrial outer membrane division [34]. Compared with the mitochondria in the control strain, the mitochondria under FIS1 overexpression exhibited normal size but larger number, and diffused towards the center of cytoplasm (Fig. 4b). Differently, LSB3 interacts with the protein associated with actin assembly [39]. Overexpression of LSB3 did not affect mitochondrial subcellular dispersion, but enlarge the volume (Fig. 4b). Meanwhile, overexpression of MBA1 and AIM25 demonstrated similar pattern, i.e. dispersed mitochondria with larger numbers (Fig. 4b). These data suggested that increase on mitochondrial number and size might make the compartmentalized sabinene synthesis pathway to better cooperate. Among these four targets significantly associated with sabinene output, overexpression of AIM25 achieved the highest sabinene production, which was 1.16-fold increase (to 90.4 mg/L) of the sabinene titer of the control stain (Fig. 4a). Further insertion of all the engineered genes including ERG20^{ww}, t34SabS1, MLS–t34SabS1 and AIM25 into the chromosome of the host strain YCTH1, boosted sabinene production to 154.9 mg/L (generating strain Sc0512020) (Fig. 4c). This titer was 58.5-fold of the one of our original stain.

Discussions

At present, engineering microorganisms as cell factory to manufacture commercial compounds has become a promising complement to traditional sources [17, 45]. The existence of sub-organelles offers eukaryotic hosts a great advantage over prokaryotic ones, due to the isolating function of organelle membranes impermeable to various chemicals. The unique eukaryotic metabolism compartmentalized in organelles not only provides favorable reaction condition and sufficient precursor supply, but also establishes an ideal place by reducing chemical consumption, removal and cytotoxicity [10, 46]. However, people are still habituated to reconstruction of heterologous metabolic pathways in cytosol of eukaryotic host, which might limit availability of precursors locating in other cellular compartments. Like in S. cerevisiae, succinyl-CoA synthesized in mitochondria is hard to be utilized as a substrate for heterologous 5-aminolevulinic acid synthase expressed in cytosol [47]. It is also reported that α-ketoisovalerate generated in mitochondria is not well conversed by cytosolic branched-chain amino acid

aminotransferases [11]. Similarly, for sabinene synthesis in this study, the N-truncated sabinene synthase was proved to be located within cytosol (Fig. 3a). And it is also revealed significant GPP pools existing in yeast membrane-bound organelles besides cytosol (Fig. 3b). Thus, the barrier by organelle membranes between the key enzyme and its substrate is a common but easily neglected issue for microbial factories. And blindly enlarge cytosolic precursor pool would result in a waste of carbon sources and limits the potential for further optimization. It is necessary to investigate the compartmentalization of both the targeted enzymes and their substrates before construction of the biosynthetic pathway.

In previous, in order to gain high production of monoterpenes in yeast, we usually performed mutagenesis and down-regulation of the wild-type ERG20 to improve cytosolic GPP supply [7, 8]. Here, we attempted to reconstitute the sabinene synthetic pathway in specific organelles to adequately utilize the GPP pools in addition to the cytosolic supply. Accordingly, we proposed a collaborative subcellular compartmentalization strategy to set a good example to improve precursor utilization as well as to enhance the compartmentalized pathway. As a result, combined target t34SabS1 into different combination of subcellular locations dramatically boosted sabinene titer. And co-expression of t34SabS1 in CM achieved significantly higher sabinene production than those generated by harnessing other combinations of subcellular locations (i.e. CP, PM and even CPM) (Fig. 3c). GPPs are synthesized in cytosol, then parts of them, which are not consumed, transfer into mitochondrial and then are converted into sabinene. The cooperation between cytosolic and mitochondrial sabinene biosynthetic pathway might re-distribute and balance of GPPs between cytosol and mitochondrial, leading to dramatically promotion on total sabinene output. It was unanticipated that the performance of the strain harboring t34SabS1 in CPM was extreme instability (Additional file 1: Fig. S4), leaving the possibility that GPP pools might not be fully utilized. We speculated that the cell burden brought by high level expression of t34SabS1 in three subcellular location might be reason for this result, which promotes us to analyze the mechanism of GPP transportation across organelle membranes in future. By improving or shutting down GPP transportation from cytosol to particular organelle(s), conversion of GPP would be concentrated in the location benefit to sabinene synthase.

Engineering organelle size and biogenesis can adjust the levels of enzyme and chemicals stored in the particular organelle, enlarging the output of the desired product [46]. In this study, overexpression of the genes involved in mitochondria morphology uncovered four novel molecular targets (i.e. FIS1, LSB3, MBA1 and AIM25) associating with sabinene output (Fig. 4a). And increasing the expression levels of this proteins did not affect the expression levels of t34SabS1 located in CM (Fig. 4a), but enlarge the mitochondrial number and size (Fig. 4c). These alternations on mitochondria morphology improved the compartmentalized sabinene synthesis pathway, which might due to the increase on GPP cargo, or to rearrangement of the subcellular distribution of GPP between cytosol and mitochondria. Coincidentally, besides the function connecting to mitochondrial morphology, these four proteins all involved the effect against cell stress. Overexpression of FIS1 can reduce accumulation of ROS (reactive oxygen species) [48] which is always represented as oxidative stress triggered by heterologous monoterpenes [49, 50]. LSB3 responses to DNA damage which is another consequence of ROS accumulation brought by the cytotoxicity of monoterpenes [51]. MBA1 displays tolerance to mistranslation-induced proteotoxic stress

[52]. And AIM25 also responses to oxidative stress. Above described function might help to relieve the cytotoxicity brought by sabinene, which might be another reason why individual overexpression of FIS1, LSB3, MBA1 and AIM25 boosted sabinene titer. Further comparative transcriptomics analysis would be helpful to investigate the molecular mechanism of these targets.

Conclusion

This study confirmed the location of N-truncated sabinene synthase in yeast cytosol and the existence of GPP pools in membrane-bound organelles like peroxisomes and mitochondria. Accordingly, we achieved a significant improvement on sabinene production based on the combination of the compartmentalized sabinene biosynthesis pathways targeted to cytosol and mitochondrial, as opposed to only cytosol. Then four novel molecular targets (i.e. FIS1, LSB3, MBA1 and AIM25) associated with mitochondria morphology were identified. And individual overexpression of these four proteins can enhance the compartmentalized pathways. Eventually, based on a fully integrated platform, simultaneously expression of t34SabS1 in cytosol and mitochondria (CM) and overexpression of AIM25 boosted sabinene titer to 154.9 mg/L which is almost 60-fold of that of our original stain. This study sets up a promising strategy to biosynthesize GPP derivatives by spatial control of the key enzyme and organization of the metabolic pathways in cells. It also provides a platform and several underlying molecular targets, with regard to microbial overproduction of monoterpenes.

Materials And Methods

Strains cultivation and product analysis

In this study, all the yeast strains engineered for sabinene production (Table 2) were derived from S. cerevisiae YJGZ1 [17] and cultured in YPD medium (2% tryptone, 1% yeast extract and 4% glucose) or in synthetic complete (SC) drop-out medium [53] at 30℃. For fermentation at shake-flask level, a single yeast colony was inoculated in 3 mL SD medium and cultured at 30 ℃, 220 rpm for 24 hours. Then the preculture was transferred into 5 mL of the same medium with an initial OD_{600} of 0.2, and cultured at 30 ℃, 220 rpm for 12–18 h. After that, the seed culture was transferred to 50 mL YPD medium with an initial OD_{600} of 0.1. In the meanwhile, 20% (v/v) IPM was added into the media. The cells were cultured at 30℃, 220 rpm for 96 hours until harvest.

Table 2

Strains used in this study

Yeast Strains	Description	Source
YJGZ1	MAT a; URA3-52, TRP1-289, LEU2-3,112, HIS3Δ1, MAL2-8C, SUC2, GAL80Δ::$P_{GAL11,10}$-IDI1, tHMGR	[17]
Sc041001	YJGZ1, pYGG415E1	This study
Sc041008	YJGZ1, pYGG415Et43	This study
Sc041009	YJGZ1, pYGG415Et34	This study
Sc041010	YJGZ1, pYGG415Et52	This study
Sc041025	YCTH1, pYGG415Et34	This study
Sc041030	YJGZ1, pCTH01	This study
Sc041031	YJGZ1, pCTH02	This study
Sc041032	YJGZ1, pCTH03	This study
Sc041033	YJGZ1, pCTH04	This study
YCTH1	YJGZ1, P_{ERG20}_ERG20 :: P_{HXT1}_ERG20	This study
Sc041055	YCTH1, pYGG415E, HO△::P_{GAL1}- t34SabS1–SKL-T_{TDH2}-KanMX	This study
Sc041056	YCTH1, pYGG415E, TRP1::TRP1-P_{GAL1}-MLS– t34SabS1-T_{TDH2}	This study
Sc041057	YCTH1, TRP1::TRP1-P_{GAL1}-MLS– t34SabS1–RFP-T_{TDH2}	This study
Sc041058	YCTH1, HO△::P_{GAL1}-RFP–t34SabS1-SKL-T_{TDH2}-KanMX	This study

'–' refers to the fusion of the proteins before and after this symbol. And 't34SabS1'refers to the sabinene synthase derived from Salvia pomifera.

Yeast Strains	Description	Source
Sc041059	Sc041057, pCTH06	This study
Sc041060	Sc041058, pCTH05	This study
Sc041063	YCTH1, pYGG415Et34, HO△::P_{GAL1}- t34SabS1–SKL-T_{TDH2}-KanMX	This study
Sc041064	YCTH1, pYGG415Et34, TRP1::TRP1-P_{GAL1}-MLS– t34SabS1-T_{TDH2}	This study
Sc041065	YCTH1, pYGG415Et34, HO△::P_{GAL1}- t34SabS1-T_{TDH2}-KanMX	This study
Sc041066	YCTH1, pYGG415E, HO△::P_{GAL1}- t34SabS1–SKL-T_{TDH2}-KanMX, TRP1::TRP1-P_{GAL1}-MLS–t34SabS1-T_{TDH2}	This study
Sc041067	YCTH1, TRP1::TRP1-P_{GAL1}-MLS– t34SabS1-T_{TDH2}, HO△::P_{GAL1}_t34SabS1–SKL-T_{TDH2}-KanMX	This study
Sc041069	YCTH1, pYGG415Et34 HO△::P_{GAL1}- t34SabS1–SKL-T_{TDH2}-KanMX, TRP1::TRP1-P_{GAL1}-MLS–t34SabS1-T_{TDH2}	This study
YJHJ1	Sc041064, URA-P_{HTX1}-ERG20△::P_{HTX1}_ERG20	This study
Sc0512001	YJHJ1, pJHJ01,	This study
Sc0512002	YJHJ1, pJHJ02,	This study
Sc0512003	YJHJ1, pJHJ03,	This study
Sc0512004	YJHJ1, pJHJ04,	This study
Sc0512005	YJHJ1, pJHJ05,	This study
Sc0512006	YJHJ1, pJHJ06,	This study

'–' refers to the fusion of the proteins before and after this symbol. And 't34SabS1'refers to the sabinene synthase derived from Salvia pomifera.

Yeast Strains	Description	Source
Sc0512007	YJHJ1, pJHJ07,	This study
Sc0512008	YJHJ1, pJHJ08,	This study
Sc0512009	YJHJ1, pJHJ09,	This study
Sc0512010	YJHJ1, pJHJ10,	This study
Sc0512011	YJHJ1, pJHJ11,	This study
YJHJ1-RFP	Sc041057, URA-P_{HTX1}-ERG20△::P_{HTX1}-ERG20 pYGG415Et34	
Sc0512012	YJHJ1-RFP, pJHJ02,	This study
Sc0512013	YJHJ1-RFP, pJHJ08,	This study
Sc0512014	YJHJ1-RFP, pJHJ10,	This study
Sc0512015	YJHJ1-RFP, pJHJ11,	This study
Sc0512016	YCTH1, URA-P_{HTX1}-ERG20△::P_{HTX1}-ERG20, pCTH03, pJHJ02, TRP1::TRP1-P_{GAL1}-MLS– t34SabS1-T_{TDH2}	This study
Sc0512017	YCTH1, URA-P_{HTX1}-ERG20△::P_{HTX1}-ERG20, pCTH03, pJHJ08, TRP1::TRP1-P_{GAL1}-MLS– t34SabS1-T_{TDH2}	This study
Sc0512018	YCTH1, URA-P_{HTX1}-ERG20△::P_{HTX1}-ERG20, pCTH03, pJHJ10, TRP1::TRP1-P_{GAL1}-MLS– t34SabS1-T_{TDH2}	This study
Sc0512019	YCTH1, URA-P_{HTX1}-ERG20△::P_{HTX1}-ERG20, pCTH03, pJHJ11, TRP1::TRP1-P_{GAL1}-MLS– t34SabS1-T_{TDH2}	This study
Sc0512020	YCTH1, HO::T_{CYC1}-P_{TDH3}-AIM25-T_{TEF1}-URA, URA::T_{ADH1}-ERG20^{ww}-$P_{GAL1,10}$-t34SabS1-T_{TDH2}-LEU, TRP1::TRP1-P_{GAL1}-MLS– t34SabS1-T_{TDH2}	This study

'–' refers to the fusion of the proteins before and after this symbol. And 't34SabS1'refers to the sabinene synthase derived from Salvia pomifera.

After that, 1 mL of organic phase was taken from the upper layer of culture and centrifuged at 12,000 rpm for 5 min. The IPM phase was diluted in hexane after dehydration and filtration. The samples were analyzed by the GC-TOF-MS system consisted of an Agilent 6890 gas chromatography (Agilent Technologies, USA) and a TOF-MS (Waters Corp., USA). Sample was injected by an Agilent 7683 autosampler into GC which equipped with a fused-silica capillary column (30 m × 0.25 mm i.d., 0.25 mm DB-5MS stationary phase, J & W Scientific, Folsom, USA). It was operated on constant pressure mode at 91 kPa. The injector temperature was 250 °C. The column effluent was introduced into the ion source (230 °C) of TOF-MS. The mass scan range was 50–800 m/z. For GC-TOF-MS analysis of sabinene, the temperature gradient program started at 50 °C for 4 min followed by heating the column at 5 °C/min to 100 °C (hold for 1 min), then increased to 250 °C at 25℃/min, holding for 5 min.

Plasmids construction and DNA manipulation

The plasmids used in this study were listed in Additional file 1: Table S1. Plasmids pYGG415 and pYGG416, which were used to construct all the cassettes utilized in this study, were individually derived from the single-copy plasmid pRS415 and pRS416 (Addgene, USA) by introducing synonymous mutations at the BsaI site within the ampicillin resistance marker. To achieve sabinene production by cytoplasmic sabinene synthase, the cassette T_{ADH1}-$P_{GAL1,10}$-T_{TDH2} were recovered from plasmid pJGZ3 [17] (Additional file 1: Table S1) by NotI digestion and cloned into pYGG415, obtaining the recombinant vector pYGG415D. The full-length sequences encoding sabinene synthase from S. pomifera (Sp_SabS1) were synthesized by Genscript Inc. (NJ, China) according to the codon bias of S. cerevisiae (Additional file 1: Fig. S7). And when expressing truncated SabS1 (tSabS1), the encoding sequences were obtained through PCR using full-length SabS1 as the template to get rid of the N-terminus plastid-targeting peptides. The (t)SabS1 products were digested by BsaI and inserted into the same site of pYGG415D, while gene $ERG20^{WW}$ was cloned into the BsmBI site, generating a series of plasmids (Additional file 1: Table S1) including the vector pYGG415E1 (Additional file 1: Fig. S1a). These plasmids harboring the expression cassettes for both (t)SabS1 and $ERG20^{WW}$ were individually transferred into the corresponding host cells using the LiAc/SS carrier DNA/PEG method. The colonies were selected on SC-LEU medium and verified by PCR with the primers listed in Additional file 1: Table S2.

In order to down-regulate endogenous ERG20, the promoter of ERG20 was replaced by that of HXT1. Promoter P_{HXT} were amplified from yeast genome and the region loxP-URA3-loxP were amplified from plasmid peasy-loxp (Additional file 1: Table S1). The PCR products were assembled by OE-PCR, obtaining the cassette loxP-URA3-loxP-P_{HXT}-ERG20. This cassette was transformed into the strain YJGZ1 (Table 2) and substituted for endogenous region P_{ERG20}-ERG20, generating strain YCTH1 (Additional file 1: Fig. S1b). The colonies were selected on SC-URA medium and verified by PCR with the primers listed in Additional file 1: Table S2. When targeting t34SabS1 into peroxisomes or mitochondria, signal peptide SKL [26] or MLS [27] was individually fused at C-terminal or N-terminal of t34SabS1 via PCR with the primers listed in Additional file 1: Table S2. Organelle-targeting sequences SKL and MLS as well as the homologous recombination arms HO-LHA/RHA and TRP1-LHA/RHA were obtained by PCR using whole-genome sequences of strain YJGZ1 [17] as the template, while promoter P_{GAL1} and terminator T_{TDH2} were

gained from plasmid pYGG415D. Marker KanMX were recovered from plasmid pRS417-Cre (Additional file 1: Table S1). These parts share 20–40 bp homologous regions with the adjacent fragments, therefore they can be assembled by overlap extension PCR (OE-PCR) (Additional file 1: Fig. S1c). The gel purified PCR products were transferred into the corresponding host cells and integrated into the HO or TRP locus. The colonies were selected on YPD-G418 or SC-TRP medium and verified by PCR with the primers listed in Additional file 1: Table S2. In order to measure the expression level of t34SabS1 as well as verify its location, red fluorescent protein (RFP) was fused at the C-terminus of t34SabS1 by OE-PCR (Additional file 1: Fig. S1d). PEX3 and COX4 are the native proteins of peroxisome and mitochondria of Saccharomyces cerevisiae [28, 29], respectively, and plasmids pCTH05 and pCTH06 were introduced into t34SabS1–RFP strains to characterize the localization effect of sabinene synthase. The following procedure was consistent with the above.

Before overexpression of the genes related to mitochondrial dynamics, the URA3 marker was deleted from strain Sc041064 via introducing plasmid pRS417-P_{GAL1}-Cre-EBD-T_{97}-KanMX into the Sc041064 strain and selecting the colonies on SC-G418-LEU medium and verified by PCR with the primers listed in Additional file 1: Table S2. A single colony of the transformants were picked up from SC-G418-LEU agar plates and inoculated into 3 mL SC-G418-LEU medium and cultivated at 30 °C, 220 rpm. After saturation, cells from 100 μL culture were collected by centrifugation at 5000 rpm, washed twice with sterile water, and transferred into 5 mL of SG-G418-LEU medium supplemented with 0.1 μL of 5 μmol/L of estrogen. After further cultured for 24 hours, cells from culture of OD_{600} = 1 were collected, washed with sterile water, and selected on SC-LEU solid medium. The colonies were verify by PCR with the primers listed in Additional file 1:Table S2.

Assay of subcellular localization and relative fluorescence (RFU)

In order to determine the subcellular localization of t34SabS1, the strains harboring RFP fused t34SabS1 were cultured in 3 mL SD medium at 30 °C, 220 rpm for 24 h. And then the seed cultures were inoculated into the same medium at initial OD_{600} of 0.2 and cultured at 30 °C, 250 rpm for 60 h (to determine subcellular localization) or 84 h (to measure expression). Cell samples were diluted into OD_{600} of 0.2–0.8, and then their RFUs were quantified by Spectra Max Series Microplate Reader (Molecular Devices, USA). The strain harbored none fluorescent protein was used as the negative control. The subcellular localization of was observed by Nikon Ti-E automatic inverted microscope (A1, Japan) equipped with a CFI Apo TIRF 100 × oil (NA 1.49) objective. Laser lines at 488, 561 nm were used for excitation. Images were processed by ImageJ and exported through NIS-Elements AR software (Nikon).

Mitochondria can also be stained to observe mitochondrial morphology as well as to confirm mitochondrial localization of t34SabS1. Cells were collected and resuspended (cell density of 10^6 cells/mL) in 50 mM sodium citrate buffer (pH 5.0) supplemented with 2% glucose. Then rhodamine 123 solution (Thermo Fisher, USA) was added into the medium with a final concentration of 30–50 μM. After incubation at 37 ℃ for 60 min, cells were harvested and then washed twice with sodium citrate buffer.

Cells were resuspended in 100 μL ddH_2O and observed by DeltaVision OMX SR Imaging System (GE Healthcare, USA). Conventional image stacks were processed by Deconvolution methods using soft WoRx (GE Healthcare, USA) with a x60/1.42 NA oil objective, solid state multimode lasers (405, 488, 568, 642 nm) and sCMOS cameras (Evolve 512 × 512, Photometrics). Serial Z-stack sectioning was done at 125 nm intervals for conventional mode.

The statistical analysis

All statistical analyses were performed with software SPSS 19.0 and the level of significance was set at $P < 0.05$. Data were collected from at least three replicate samples.

Abbreviations

IPP: isopentenyl pyrophosphate; DMAPP: dimethyl allyl pyrophosphate (DMAPP); GPP: geranyl diphosphate; NPP: neryl diphosphate; FPP: farnesyl diphosphate; ERG20: farnesyl diphosphate synthase; $ERG20^{WW}$: $ERG20^{F96W/N127W}$; C: cytosol; P: peroxisomes; M: mitochondria; CM: cytosol and mitochondria; CP: cytosol and peroxisomes; PM: peroxisomes and mitochondria; CPM: cytosol, peroxisomes and mitochondria; SabS1: sabinene synthase; t34SabS1: the sabinene synthase truncated at R43; IPM: isopropyl myristate; RFU: relative fluorescence units.

Declarations

Acknowledgement

We thank the staffs from College of Life Sciences, Nankai University and Technology Center for Protein Sciences, Tsinghua University, especially Dr. Li Jiao (Nankai University) and Dr. Yalan Chen for the assistance with Confocal Microscopy.

Authors' contributions

H-JJ, T-HC and YW conceived of the study and drafted the manuscript. H-JJ and T-HC performed the experiments. J-Z Qu constructed the plasmids for the fluorescence assay of subcellular localization. W-HX and M-D Y helped to analyze the data and draft the manuscript. CL and Y-JY participated in coordination of the study. YW supervised the whole research and revised the manuscript. All authors read and approved the final manuscript.

Funding

This work was supported by the financial support from the Natural Science Foundation of China (21621004 and 21676192).

Availability of data and materials

All data generated or analyzed during this study are included in this article.

Ethics approval and consent to participate

Not applicable.

Consent for publication

Not applicable.

Competing interests

The authors declare that they have no competing interests.

References

1. Carroll A L, Desai S H, Atsumi S. Microbial production of scent and flavor compounds. Curr Opin Biotech. 2016; 37:8-15.
2. Cuellar M C, van der Wielen L A. Recent advances in the microbial production and recovery of apolar molecules. Curr Opin Biotechnol. 2015; 33:39-45.
3. Jongedijk E, Cankar K, Buchhaupt M, Schrader J, Bouwmeester H, Beekwilder J. Biotechnological production of limonene in microorganisms. Appl Microbiol Biot. 2016; 100(7):2927-38.
4. Ignea C, Raadam M H, Motawia M S, Makris A M, Vickers C E, Kampranis S C. Orthogonal monoterpenoid biosynthesis in yeast constructed on an isomeric substrate. Nat. Commun. 2019; 10(1):3799-813.
5. Yee D A, DeNicola A B, Billingsley J M, Creso J G, Subrahmanyam V, Tang Y. Engineered mitochondrial production of monoterpenes in *Saccharomyces cerevisiae*. Metab Eng. 2019; 55:76-84.
6. Anderson M S, Yarger J G, Burck C L, Poulter C D. Farnesyl diphosphate synthetase. Molecular cloning, sequence, and expression of an essential gene from *Saccharomyces cerevisiae*. J. Biol Chem. 1989; 264(32):19176-84.
7. Ignea C, Pontini M, Maffei M E, Makris A M, Kampranis S C. Engineering monoterpene production in yeast using a synthetic dominant negative geranyl diphosphate synthase. Acs Synth. Biol. 2014; 3(5):298-306.
8. Zhao J, Li C, Zhang Y, Shen Y, Hou J, Bao X. Dynamic control of ERG20 expression combined with minimized endogenous downstream metabolism contributes to the improvement of geraniol production in *Saccharomyces cerevisiae*. Microb. Cell Fact. 2017; 16(1):17-27.
9. Peng B, Nielsen L K, Kampranis S C, Vickers C E. Engineered protein degradation of farnesyl pyrophosphate synthase is an effective regulatory mechanism to increase monoterpene production in *Saccharomyces cerevisiae*. Metab Eng. 2018; 47:83-93.
10. Hammer S K, Avalos J L. Harnessing yeast organelles for metabolic engineering. Nat. Chem. Biol. 2017; 13(8):823-32.

11. Avalos J L, Fink G R, Stephanopoulos G. Compartmentalization of metabolic pathways in yeast mitochondria improves the production of branched-chain alcohols. Nat Biotechnol. 2013; 31(4):335-41.
12. Farhi M, Marhevka E, Masci T, Marcos E, Eyal Y, Ovadis M *,et al*. Harnessing yeast subcellular compartments for the production of plant terpenoids. Metab Eng. 2011; 13(5):474-81.
13. Yuan J, Ching C. Mitochondrial acetyl-CoA utilization pathway for terpenoid productions. Metab Eng. 2016; 38:303-9.
14. Bohlmann J, Meyer-Gauen G, Croteau R. Plant terpenoid synthases: molecular biology and phylogenetic analysis. P. Natl Acad Sci Usa. 1998; 95(8):4126-33.
15. Turner G, Gershenzon J, Nielson E E, Froehlich J E, Croteau R. Limonene synthase, the enzyme responsible for monoterpene biosynthesis in peppermint, is localized to leucoplasts of oil gland secretory cells. Plant Physiol. 1999; 120(3):879-86.
16. Jongedijk E, Cankar K, Ranzijn J, van der Krol S, Bouwmeester H, Beekwilder J. Capturing of the monoterpene olefin limonene produced in *Saccharomyces cerevisiae*. Yeast. 2014; 32:159-71.
17. Jiang G, Yao M, Wang Y, Zhou L, Song T, Liu H *,et al*. Manipulation of GES and ERG20 for geraniol overproduction in *Saccharomyces cerevisiae*. Metab Eng. 2017; 41:57-66.
18. Duport C, Schoepp B, Chatelain E, Spagnoli R, Dumas B, Pompon D. Critical role of the plasma membrane for expression of mammalian mitochondrial side chain cleavage activity in yeast. Febs J. 2003; 270(7):1502-14.
19. Jiang Y, Proteau P, Poulter D, Ferro-Novick S. BTS1 Encodes a Geranylgeranyl Diphosphate Synthase in *Saccharomyces cerevisiae*. J. Biol Chem. 1995; 270(37):21793-9.
20. Valente J, Zuzarte M, Gonçalves M J, Lopes M C, Cavaleiro C, Salgueiro L *,et al*. Antifungal, antioxidant and anti-inflammatory activities of *Oenanthe crocata L*. essential oil. Food Chem Toxicol. 2013; 62:349-54.
21. Cao Y, Zhang H, Liu H, Liu W, Zhang R, Xian M *,et al*. Biosynthesis and production of sabinene: current state and perspectives. Appl Microbiol Biot. 2018; 102(4):1535-44.
22. Anita A, Julia S, A. P B, J. M A, G. P G,W. D I *,et al*. Distinct redox regulation in sub-cellular compartments in response to various stress conditions in *Saccharomyces cerevisiae*. Plos One. 2013; 8(6):e65240.
23. Liu G, Li T, Zhou W, Jiang M, Tao X, Liu M *,et al*. The yeast peroxisome: A dynamic storage depot and subcellular factory for squalene overproduction. Metab Eng. 2020; 57:151-61.
24. Orij R, Postmus J, Ter Beek A, Brul S, Smits G J. In vivo measurement of cytosolic and mitochondrial pH using a pH-sensitive GFP derivative in *Saccharomyces cerevisiae* reveals a relation between intracellular pH and growth. Microbio. 2009; 155(1):268-78.
25. Yang K, Qiao Y, Li F, Xu Y, Yan Y, Madzak C *,et al*. Subcellular engineering of lipase dependent pathways directed towards lipid related organelles for highly effectively compartmentalized biosynthesis of triacylglycerol derived products in *Yarrowia lipolytica*. Metab Eng. 2019; 55:231-8.

26. Sheng J, Stevens J, Feng X. Pathway compartmentalization in peroxisome of *Saccharomyces cerevisiae* to produce versatile medium chain fatty alcohols. Sci. Rep.-Uk. 2016; 6(1).
27. Lv X, Wang F, Zhou P, Ye L, Xie W, Xu H *,et al*. Dual regulation of cytoplasmic and mitochondrial acetyl-CoA utilization for improved isoprene production in *Saccharomyces cerevisiae*. Nat. Commun. 2016; 7(1):12851-62.
28. Huh W, Falvo J V, Gerke L C, Carroll A S, Howson R W, Weissman J S *,et al*. Global analysis of protein localization in budding yeast. Nature. 2003; 425(6959):686-91.
29. Maarse A C, Van Loon A P, Riezman H, Gregor I, Schatz G, Grivell L A. Subunit IV of yeast cytochrome c oxidase: cloning and nucleotide sequencing of the gene and partial amino acid sequencing of the mature protein. Embo J. 1984; 3(12):2831-7.
30. Kohlhaw G B. Leucine Biosynthesis in Fungi: Entering Metabolism through the Back Door. Microbiol Mol Biol R. 2003; 67(1):1-15.
31. Zhou Y J, Buijs N A, Zhu Z, Gómez D O, Boonsombuti A, Siewers V *,et al*. Harnessing yeast peroxisomes for biosynthesis of fatty-acid-derived biofuels and chemicals with relieved side-pathway competition. J. Am Chem Soc. 2016; 138(47):15368-77.
32. Merz S, Hammermeister M, Altmann K, Dürr M, Westermann B. Molecular machinery of mitochondrial dynamics in yeast. Biol Chem. 2007; 388(9).
33. Westermann B. Molecular machinery of mitochondrial fusion and fission. J. Biol Chem. 2008; 283(20):13501-5.
34. Mozdy A D, McCaffery J M, Shaw J M. Dnm1p GTPase-mediated mitochondrial fission is a multi-step process requiring the novel integral membrane component Fis1p. J. Cell Biol. 2000; 151(2):367-80.
35. Wong E D, Wagner J A, Gorsich S W, McCaffery J M, Shaw J M, Nunnari J. The dynamin-related GTPase, Mgm1p, is an intermembrane space protein required for maintenance of fusion competent mitochondria. J. Cell Biol. 2000; 151(2):341-52.
36. Meisinger C, Pfannschmidt S, Rissler M, Milenkovic D, Becker T, Stojanovski D *,et al*. The morphology proteins Mdm12/Mmm1 function in the major beta-barrel assembly pathway of mitochondria. Embo J. 2007; 26(9):2229-39.
37. Sanz P. Snf1 protein kinase: a key player in the response to cellular stress in yeast. Biochem Soc T. 2003; 31(Pt 1):178.
38. Winter D, Podtelejnikov A V, Mann M, Li R. The complex containing actin-related proteins Arp2 and Arp3 is required for the motility and integrity of yeast actin patches. Curr Biol. 1997; 7(7):519-29.
39. Madania A, Dumoulin P, Grava S, Kitamoto H, Scharer-Brodbeck C, Soulard A *,et al*. The *Saccharomyces cerevisiae* homologue of human Wiskott-Aldrich syndrome protein Las17p interacts with the Arp2/3 complex. Mol Biol Cell. 1999; 10(10):3521-38.
40. Fehrenbacher K L, Boldogh I R, Pon L A. A Role for Jsn1p in recruiting the Arp2/3 complex to mitochondria in budding yeast. Mol Biol Cell. 2005; 16(11):5094-102.

41. Frederick R L, McCaffery J M, Cunningham K W, Okamoto K, Shaw J M. Yeast Miro GTPase, Gem1p, regulates mitochondrial morphology via a novel pathway. The Journal of Cell Biology. 2004; 167(1):87-98.
42. Möller-Hergt B V, Carlström A, Stephan K, Imhof A, Ott M. The ribosome receptors Mrx15 and Mba1 jointly organize cotranslational insertion and protein biogenesis in mitochondria. Mol Biol Cell. 2018; 29(20):2386-96.
43. Hess D C, Myers C L, Huttenhower C, Hibbs M A, Hayes A P, Paw J *,et al*. Computationally driven, quantitative experiments discover genes required for mitochondrial biogenesis. Plos Genet. 2009; 5(3):e1000407.
44. Johnson L V, Walsh M L, Chen L B. Localization of mitochondria in living cells with rhodamine 123. P. Natl Acad Sci Usa. 1980; 77(2):990-4.
45. Liu H, Cheng T, Zou H, Zhang H, Xu X, Sun C *,et al*. High titer mevalonate fermentation and its feeding as a building block for isoprenoids (isoprene and sabinene) production in engineered *Escherichia coli*. Process Biochem. 2017; 62:1-9.
46. Chen R, Yang S, Zhang L, Zhou Y J. Advanced strategies for production of natural products in yeast. iScience. 2020; doi: 10.1016/j.isci.2020.100879.
47. Baldi N, Dykstra J C, Luttik M A H, Pabst M, Wu L, Benjamin K R *,et al*. Functional expression of a bacterial α-ketoglutarate dehydrogenase in the cytosol of Saccharomyces cerevisiae. Metab Eng. 2019; 56:190-7.
48. Kitagaki H, Araki Y, Funato K, Shimoi H. Ethanol-induced death in yeast exhibits features of apoptosis mediated by mitochondrial fission pathway. Febs Lett. 2007; 581(16):2935-42.
49. Beatriz C, Rafael P, Diego G, Martin P. Differential mechanism of *Escherichia coli* Inactivation by (+)-limonene as a function of cell physiological state and drug's concentration. Plos One. 2014; 9(4):e94072.
50. Liu J, Zhu Y, Du G, Zhou J, Chen J. Response of *Saccharomyces cerevisiae* to D-limonene-induced oxidative stress. Appl Microbiol Biot. 2013; 97(14):6467-75.
51. Tkach J M, Yimit A, Lee A Y, Riffle M, Costanzo M, Jaschob D *,et al*. Dissecting DNA damage response pathways by analysing protein localization and abundance changes during DNA replication stress. Nat Cell Biol. 2012; 14(9):966-76.
52. Vargas Möller-Hergt B, Carlström A, Suhm T, Ott M. Insertion defects of mitochondrially encoded proteins burden the mitochondrial quality control system. Cells-Basel. 2018; 7(10):172.
53. Su W, Xiao W H, Wang Y, Liu D, Zhou X, Yuan Y J. Alleviating redox imbalance enhances 7-dehydrocholesterol production in engineered *Saccharomyces cerevisiae*. Plos One. 2015; 10(6):e130840.

Supplementary Information

Additional file 1: Fig. S1 Schematic diagram of plasmids construction and DNA manipulation in this study. Fig. S2 The GC-TOF-MS profile of sabinene standard, the control strain and sabinene producing strain. Fig. S3 Predicted disorder structure of sabinene synthase. Fig. S4Sabinene output for sabinene synthase combined targeting to different location combination. Fig. S5 Effects of overexpression of ten proteins associated with mitochondrial dynamics on sabinene production. Fig. S6 Cell growth of strains with overexpression of FIS1, LSB3, MBA1 and AIM25. Fig. S7 Codon-optimized Salvia pomifera sabinene synthase involved in this study. Table S1. Plasmids used in this study. Table S2. Primers used in this study.

Figures

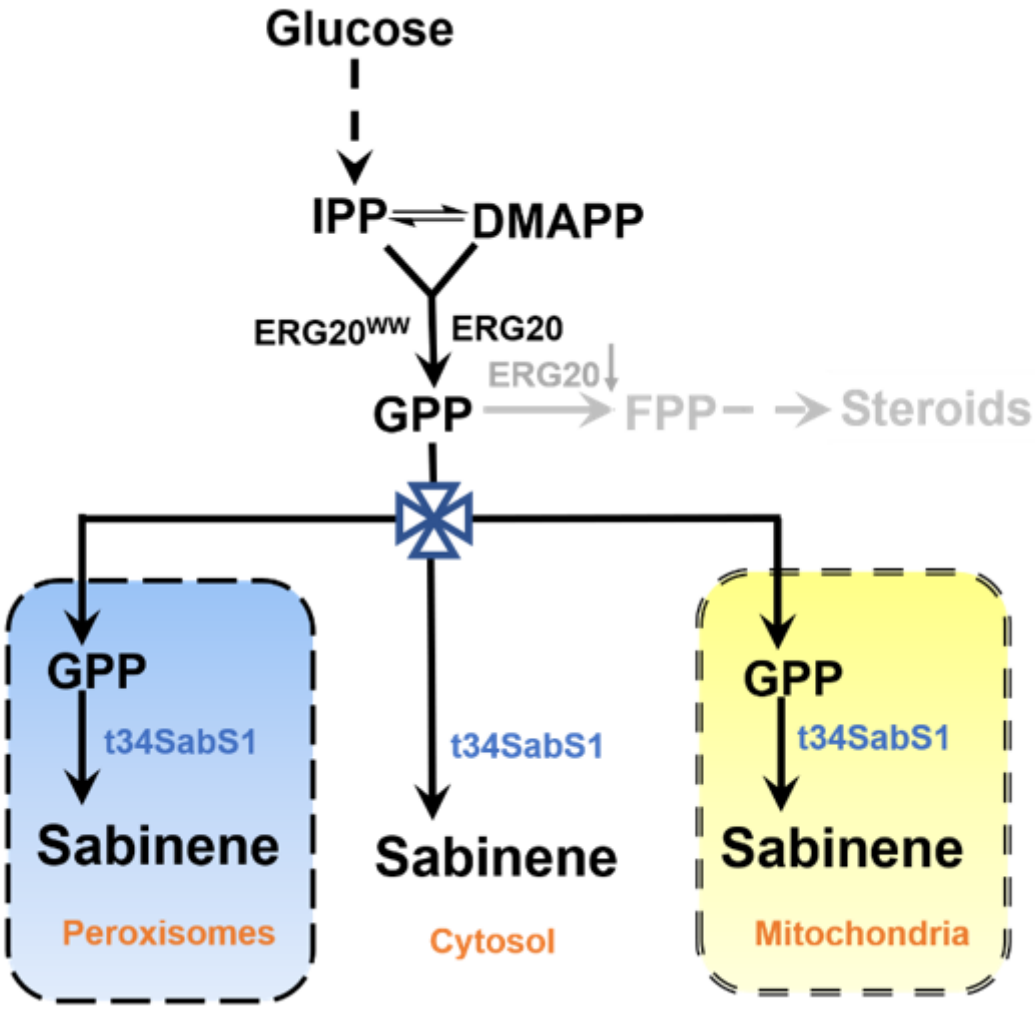

Figure 1

Overview of the engineer strategy for sabinene overproduction in yeast. The sabinene biosynthesis pathway is illustrated and the compartmentalized part are boxed by monolayer or bilayer dotted line which presents the membrane of peroxisomes or mitochondria, respectively. The communicating vessels

indicate the distribution of GPP generated in cytosol. The endogenous protein is presented by black, while the only heterologous protein is highlighted by blue. t34SabS1 is for sabinene synthase truncated at L34. ERG20WWis for ERG20 mutagenesis at F96W/N127W which weaken the activity of FPP synthase. The down arrow suggests protein down-regulation. And the down-regulated metabolic flux was marked by grey.

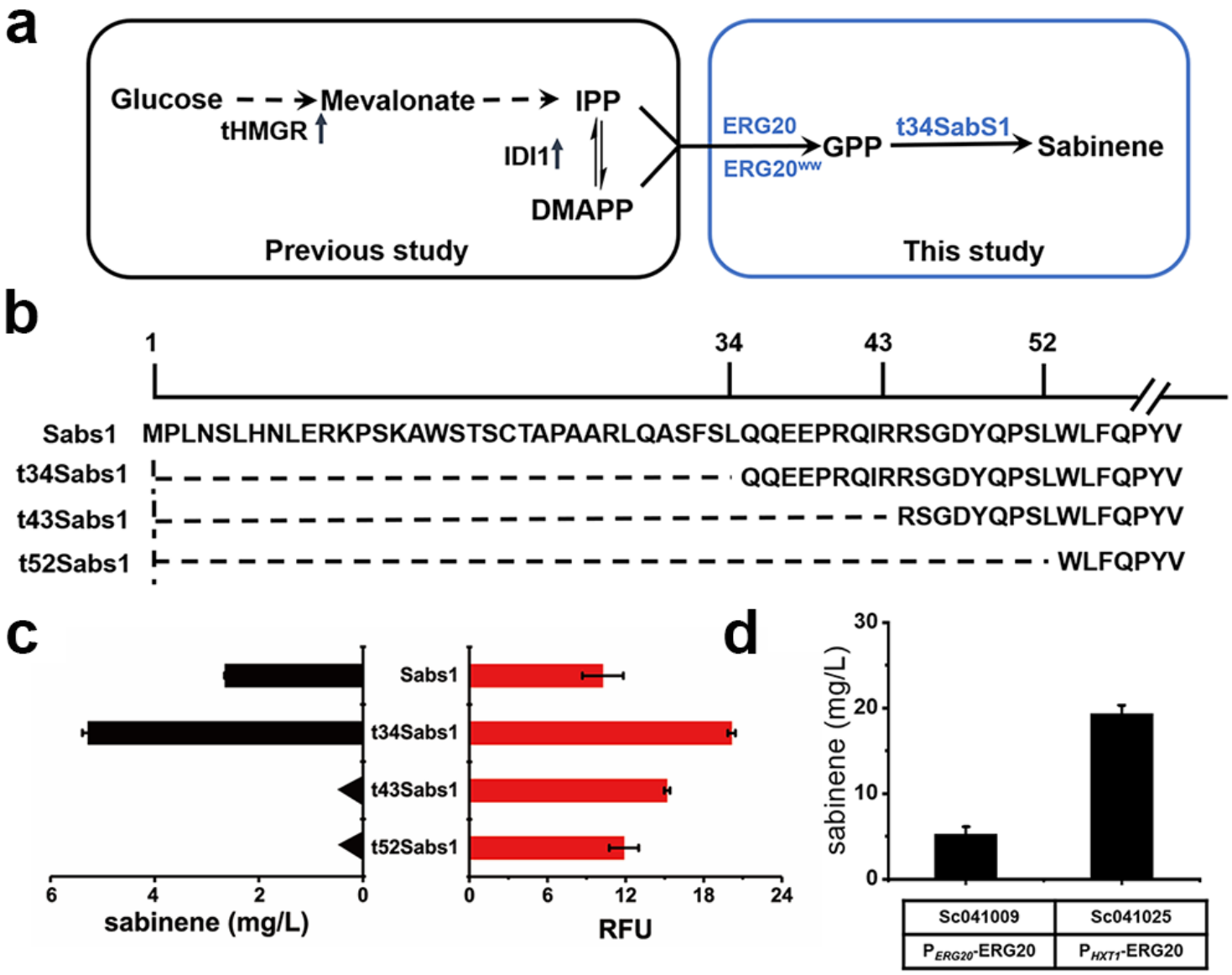

Figure 2

Construction of sabinene biosynthesis pathway in the cytosol of S. cerevisiae. a Overview of the strategy to establish sabinene biosynthesis pathway. The sabinene biosynthesis pathway is illustrated and the part involved in our previous work is marked by black and boxed by black line. The part engineered in this study is boxed by blue line and the involved proteins are presented by blue. The up arrow indicates protein up-regulation, while the down arrow suggests protein down-regulation. b Schematic of the truncated position within the N-terminus of sabinene synthase. c Effects of different truncation position within the N-terminus of sabinene synthase on their expression level and sabinene production. The

expression level of sabinene synthase was determined by the fluorescence signal intensity of RFP per OD600 (relative fluorescence units, RFU) in each strain. d Effects of down-regulation of the wild-type ERG20 on sabinene production.

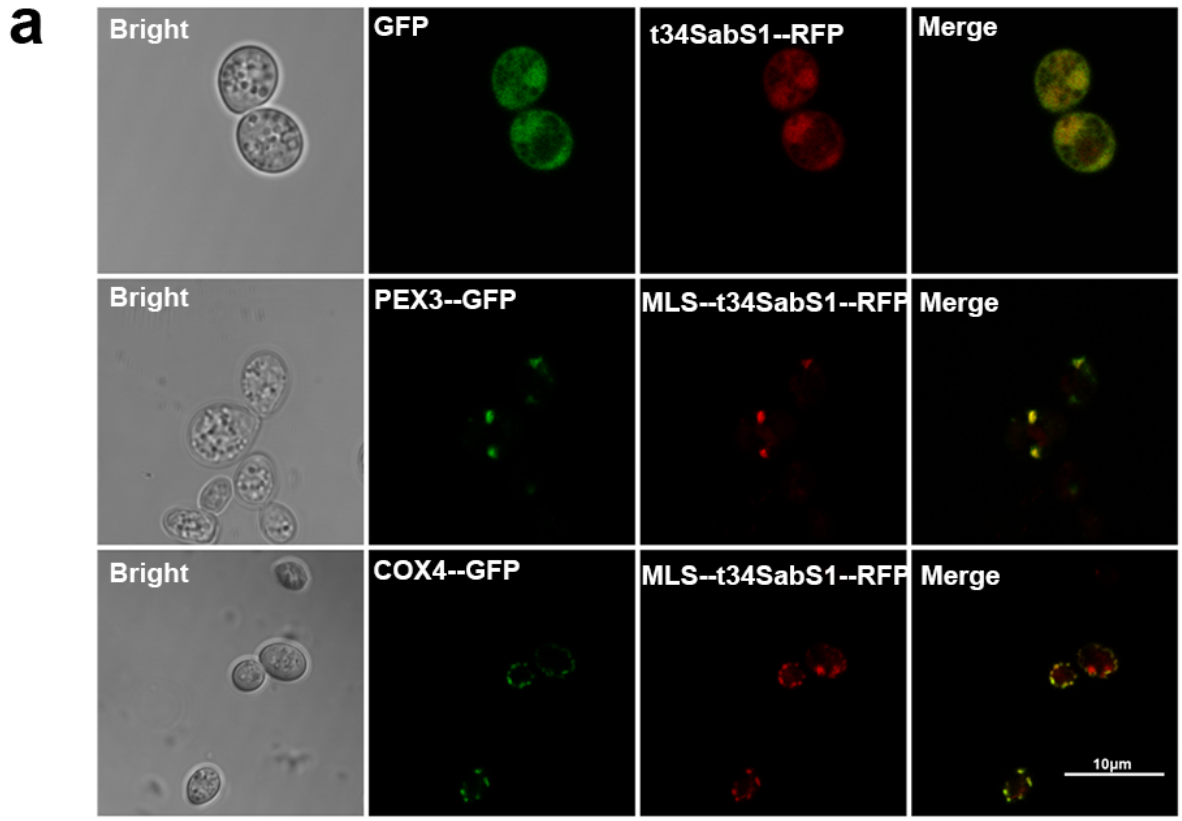

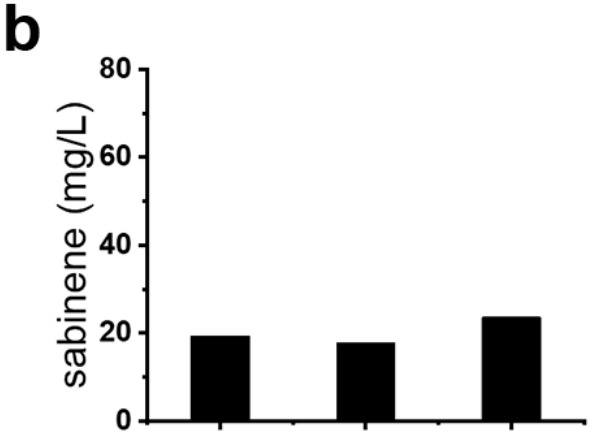

Strain	Sc04 1025	Sc04 1055	Sc04 1056
C	+		
P		+	
M			+

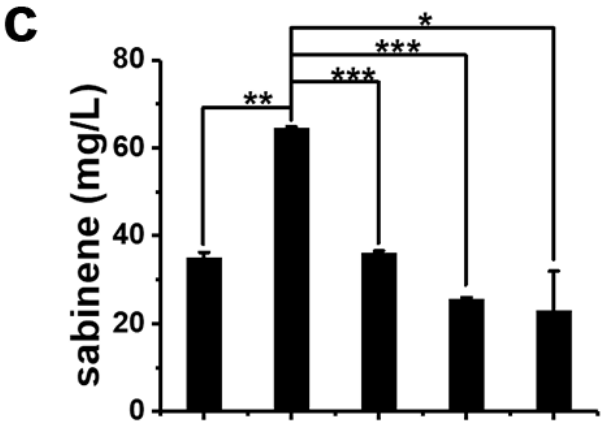

Strain	Sc0 410 63	Sc0 410 64	Sc0 410 66	Sc0 410 65	Sc0 410 67
C	+	+		++	
P	+		+		
M		+	+		++

Figure 3

Compartmentation of sabinene synthase in diversity combinations of subcellular locations. a Analysis of subcellular location of sabinene synthase (t34SabS1). PEX3 and COX4 are the specific marks presents

peroxisomes and mitochondria, respectively. SKL or MLS are protein-targeting signals directing proteins towards peroxisomes and mitochondria, respectively. '–' refers to the fusion of the proteins before and after this symbol. b Sabinene production of strains with t34SabS1 individually targeting towards single subcellular location. c Sabinene production of strains with t34SabS1 individually targeting towards double subcellular location. C, cytosol; P, peroxisomes; M, mitochondria. * is for p <0.05, ** is for p <0.01 and *** is for p <0.001.

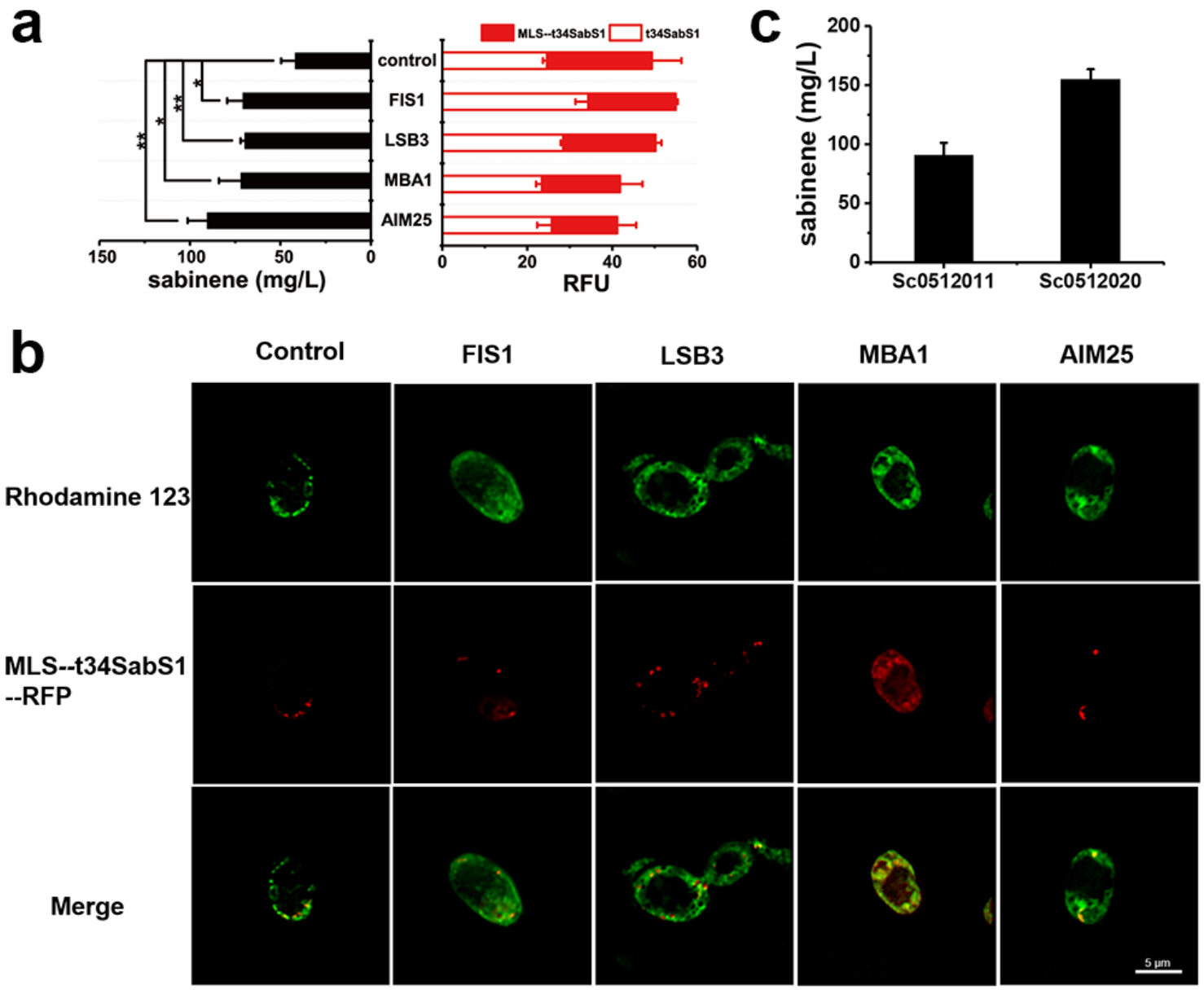

Figure 4

Tuning mitochondria morphology. a The effect of overexpressing proteins associated with mitochondria dynamics on sabinene production and expression level of sabinene synthases. t34SabS1 and MLS–t34SabS1 are for sabinene synthases expressed in cytosol and mitochondria, respectively. '–' refers to the fusion of the proteins before and after this symbol. The expression level of sabinene synthase expressed in cytosol or mitochondria was determined by the fluorescence signal intensity of RFP per OD600 (relative fluorescence units, RFU) in each strain. *, p <0.05; **, p <0.01. b Mitochondria morphology of strains after

overexpressing the target. Rhodamine 123 specific dyes yeast mitochondria. c Sabinene production of strain constructed based on a fully integrated platform.

Supplementary Files

This is a list of supplementary files associated with this preprint. Click to download.

- SupplemantaryMeteria.docx